

Journal Pre-proof

Flash flood susceptibility assessment using the parameters of drainage basin morphometry in SE Bangladesh

Akhtar Alam, Bayes Ahmed, Peter Sammonds



PII: S1040-6182(20)30221-4

DOI: <https://doi.org/10.1016/j.quaint.2020.04.047>

Reference: JQI 8275

To appear in: *Quaternary International*

Received Date: 25 March 2020

Revised Date: 27 April 2020

Accepted Date: 29 April 2020

Please cite this article as: Alam, A., Ahmed, B., Sammonds, P., Flash flood susceptibility assessment using the parameters of drainage basin morphometry in SE Bangladesh, *Quaternary International* (2020), doi: <https://doi.org/10.1016/j.quaint.2020.04.047>.

This is a PDF file of an article that has undergone enhancements after acceptance, such as the addition of a cover page and metadata, and formatting for readability, but it is not yet the definitive version of record. This version will undergo additional copyediting, typesetting and review before it is published in its final form, but we are providing this version to give early visibility of the article. Please note that, during the production process, errors may be discovered which could affect the content, and all legal disclaimers that apply to the journal pertain.

© 2020 Published by Elsevier Ltd.

1 **Flash flood susceptibility assessment using the parameters of drainage basin morphometry**
2 **in SE Bangladesh**

3 Akhtar Alam^{1*}, Bayes Ahmed¹, Peter Sammonds¹

4 ¹Institute for Risk and Disaster Reduction, University College London, Gower Street, London,
5 WC1E 6BT, United Kingdom.

6

7 *Corresponding author: AA (akhtar.alam@ucl.ac.uk)

8

9 **Abstract**

10

11 Predicting the occurrence and spatial patterns of rainfall induced flash floods is still a challenge.

12 Instant genesis and typically smaller areal coverage of the flash floods are the major

13 impediments to their forecasting. Analysis of the morphometric parameters provides useful

14 insight on hydrological response of the drainage basins to high intensity rainfall events. This

15 information is valuable for understanding the flash flood potential of the drainage basins and for

16 evading the destructions caused by the hazard. Here, we use eighteen morphometric parameters

17 that influence the runoff volume, flow velocity, and inundation depth scenario of a flash flood.

18 The analysis has been carried out for simulating the relative flash flood susceptibility of thirteen

19 watersheds (B1 to B13) of variable sizes in southeastern Bangladesh. The morphometric

20 parameters were derived from Digital Elevation Model (DEM) using Geographic Information

21 System (GIS). The evaluated basin parameters include: area (A), perimeter (P), length (Lb),

22 stream order (Su), stream number (Nu), stream length (Lu), stream frequency (Fs), drainage

23 density (Dd), texture ratio (Rt), bifurcation ratio (Rb), basin relief (Hr), relief ratio (Rr),

24 ruggedness number (Rn), time of concentration (Tc), infiltration number (If), and form factor

25 (F). Two relative flash flood susceptibility scenarios were generated: (i) general watershed level,

26 and (ii) more precise pixel level status. The watershed level comparison reveals that B4 and B6

27 watersheds constituting 72.61% of the total area are 'very high' susceptible, whereas the

28 susceptibility of the other watersheds has been found as 'high' [B5 (6.95%)], 'moderate' [B8 and
29 B13 (8.63%)], 'low' [B2, B10, B11 (4.64%)], and 'very low' [B1, B3, B7, B9, and B12
30 (7.18%)]. The derived watershed susceptibility map was subsequently integrated with two spatial
31 analysis algorithms i.e., topographic wetness index (TWI) and topographic position index (TPI)
32 through overlay analysis. The integration helped to understand the combined role of the general
33 watershed morphometry and the in situ topography for determining flash flood susceptibility of
34 each spot (30m x 30m) within all the selected watersheds. The quantitative analysis and
35 characterization of the watersheds from the perspective of flash flood hazard in this investigation
36 is expected to be useful for implementing the site-specific mitigation measures and alleviating
37 the effects of the hydrological hazard in the study area.

38 **Keywords:** basin; drainage; flash floods; morphometry; Bangladesh; Remote sensing; GIS

39

40 1. Introduction

41 Flash floods are among the world's deadliest natural hazards, accounting for 85% of flooding,
42 having the highest mortality rate with more than 5,000 lives lost annually (www.wmo.int).
43 Bangladesh is one of the most flood prone countries in the world experiencing almost all types
44 of flooding. Having a long history of the hydrometeorological disasters, the country has
45 witnessed a huge clustering of the extreme flood events in close space and time. The most
46 devastating flood events of 1953, 1954, 1955, 1956, 1962, 1963, 1966, 1968, 1969, 1970,
47 1971, 1974, 1976, 1984, 1987, 1988, 1997, 1998, 2000, 2004, 2007 and 2012 are examples of the
48 series from the 20th and beginning of the 21st century (Khalil, 1990; Dewan et al., 2003;
49 Choudhury and Haque, 2016; Philip et al., 2019). The impact of the most recent monsoon flood
50 in 2019 has also been widespread, effecting 2.1 million people in 24 districts and killing 104

51 people (BRCS, 2019; www.dhakatribune.com). On an average floods inundate 20.5% area of the
52 country annually to as high as about 70% during an extreme flood event, primarily because of
53 the low-lying topography and location of the country at the confluence of three major rivers i.e.,
54 Ganges, Brahmaputra and Meghna (Mirza, 2002). The floodplains of these rivers constitute
55 about 80% area of the country; however, more than 90% of the catchment area of these rivers is
56 outside Bangladesh (Brammer, 1990).

57 Flash floods, although affecting relatively lesser area (5-20%), result in substantial loss of human
58 lives, property, and livelihoods especially in the mountainous parts of the country (Kamal, 2018).
59 In a recent flash flood of August 2014, around 0.81 million people were affected, including 0.5
60 million displaced, and thousands of hectares of crops lost (ACAPS, 2014). This was immediately
61 followed by another flash flood in June 2015, hitting southeastern parts of the country; Cox's
62 Bazar, Bandarban, and Chittagong districts were severely affected by this flash flood in which 22
63 persons were killed and 1.8 million people effected (HCTT, 2015). Another high intensity
64 rainfall triggered flash flood was experienced during April 2017; the breaching of embankments
65 from this event resulted in inundation of extensive cropland mainly in six northern districts and
66 effected more than 4.6 million people (Tarannum, 2018). A heavy downpour in June 2018
67 recorded over 300 mm of rain in just 48 hours destroying hundreds of Rohingya refugee shelters
68 in the Cox's Bazar district (www.floodlist.com).

69 Flash floods are mostly of convective origin, occurring locally in watersheds of less than
70 1000 km² with complex orography and short response times of few hours or minutes; thus,
71 allowing minimum possibilities for the prediction (Marchi et al., 2010; Destro et al., 2018).
72 Usually taking place in ungauged watersheds, flash floods are the least documented phenomenon
73 of the hydrometeorology (Gaume et al., 2009). While, torrential rainfall remains the main reason

74 behind the occurrence of the flash floods, watershed morphometry is an important factor
75 influencing the intensity of the hazard. Characterizing the morphometric properties of the
76 catchments provide a valuable insight about their hydrological response (e.g., flash flood) to
77 rainfall events (Borga et al., 2008).

78 The classic works of Horton, 1932 and 1945, Smith, 1950; Strahler 1952, Miller, 1953 and
79 Schumm, 1956 have long been used as a guide for such studies. In the recent years, quantitative
80 analysis of the morphometric properties [linear, areal, and relief] of the basin through the
81 application of mathematical measures has been widely performed for multiple purposes
82 especially for assessing flood hazard potential of the drainage basins (e.g., Mesa, 2006;
83 Angillieri, 2008; Ozdemir and Bird, 2009; Romshoo et al., 2012; Bhatt and Ahmed, 2014;
84 Abuzied et al., 2016; Farhan et al., 2015; Fenta et al., 2017; Bhat, 2019, Adnan et al., 2019).

85 Remote sensing data products and Geographic Information System (GIS) have often been
86 integral part of the studies performing spatial assessment of various natural hazards and other
87 processes operating on the earth (Alam et al., 2018, 2019b; Ahmed et al., 2020). Freely available
88 the digital elevation models (DEMs) such as Shuttle Radar Topography Mission (SRTM),
89 Advanced Spaceborne Thermal Emission and Reflection Radiometer (ASTER) and Advanced
90 Land Observing Satellite (ALOS) in combination with GIS have been particularly used for
91 drainage basin morphometric analysis (e.g., Reddy et al., 2004; Romshoo et al., 2012; Altaf et
92 al., 2013; Bhatt and Ahmed 2014; Farhan et al., 2015; Adnan et al., 2019; Bhat et al., 2019,
93 Meraj et al., 2019).

94 Quantitative morphometric analysis of the selected basins in the present study is particularly
95 important because the basins are ungauged and there is lack of information on their past
96 hydrological behavior. Accordingly, with the combined use of digital elevation data (SRTM)

97 and GIS, this study attempts to evaluate eighteen discharge, flow velocity, and inundation
98 influencing morphometric parameters i.e., area (A), perimeter (P), length (Lb), stream order (Su),
99 stream number (Nu), stream length (Lu), stream frequency (Fs), drainage density (Dd), texture
100 ratio (Rt), bifurcation ratio (Rb), basin relief (Hr), relief ratio (Rr), ruggedness number (Rn), time
101 of concentration (Tc), infiltration number (If), form factor (F), topographic wetness index (TWI)
102 and topographic position index (TPI) for assessing the flash flood susceptibility of the selected
103 watersheds/basins.

104 **2. Study area**

105 The area of interest is located between 21°00'0" – 21°60'0" N and 92°05'0" – 92°35'0" E in the
106 southeastern Bangladesh. (Fig 1). The total area of the selected site is 3170 km², spread over the
107 parts of multiple *Upazilas* in three districts i.e., Cox's Bazar [Chakaria, Cox's Bazar-S, Ramu,
108 Ukhia and Teknaf] Bandarban [Alikadam, Naikhongchhari and Lama], and relatively small part
109 of Chittagong [Banskhali]. The area is composed of 13 watersheds/basins (B1, B2,..B13) with
110 sizes ranging from 16.8 km² (B11) to 1525.4 km² (B4) and being a coastal area elevation
111 stretches from 0 to 889 meters above mean sea level. The eastern segment of the study area
112 encompasses high mountainous, with steep slopes and higher drainage density (see Fig 2 for
113 general geomorphic properties of the area). Surface geology of the region consists of beach and
114 dune sand (Coastal sediments), valley alluvium and colluvium, Dihing and Dupi Tila Formation,
115 Dihing Formation (Pleistocene and Pliocene), Tipam Sandstone (Neogene), Boka Bil Formation
116 (Neogene) and Bhuban Formation (Miocene) (GSB, 1990). The geomorphic signatures are
117 evocative of NW-SE trending geological structures controlling the watercourses e.g., the trunk
118 channel in the watershed B4 of the study area. Rainfall in the area exhibits a specific spatial
119 pattern; the southern watersheds receive relatively higher mean annual rainfall than the northern
120
121

122 watersheds (Fig. 2e). The area is often experiencing the flash floods and consequent losses
123 especially during the monsoon season; the most recent events have been those of 2015 and 2018.
124 It important to note that in addition to the native population, there are 209,847 Rohingya refugee
125 families with a population of 909,774 (UNHCR, 2019) temporarily settled in the watershed B9,
126 B10, B11, and B13 (since August, 2017), who now become the prey of the flash floods (e.g., in
127 2018). The refugees are living in makeshift tarpaulin and bamboo shelters spread over the
128 multiple clusters in Ukhia and Teknaf *Upazilas* of the Cox's Bazar district. Given the occurrence
129 of varied natural hazards including cyclones, landslides and floods (Ahmed et al., 2018; Alam et
130 al., 2019) and social, economic and demographic conditions, the refugees seem to be the most at-
131 risk community in the study area.

132 **3. Materials and methods**

133 Quantitative analysis of the morphometric parameters has long been used to understand the
134 nature and origin of the drainage basins (Horton 1945, Smith, 1950; Strahler 1952, Miller, 1953
135 and Schumm, 1956). The morphometric characteristics considerably impact the hydrological
136 behavior of the catchments; consequently, number of previous investigations have been carried
137 out in relation to the flood hazard. Drainage basin morphometry can play a substantial role in the
138 occurrence and intensity of the flash floods (Fig 3). Over the period of time, morphometric
139 parameters have been widely used for understanding the relationship; however, there is no
140 defined or standard set of the morphometric parameters that may be used for flash flood
141 susceptibility analysis (Adnan et al., 2019). In most of the previous studies, the results obtained
142 through the process of morphometric analysis tend to be generalized, where discharge generating
143 potential or response to rainfall events is projected relatively between the various watersheds
144 without the identification of hazard-hotspots. The deliverables of such studies are of limited use
145

146 from the perspective of flood hazard mitigation. For that reason, the present study adopted a two-
147 step approach to assess the flash flood susceptibility of the study area. The 1st step aims to
148 understand relative flood hazard scenario of the watersheds by deriving the values of each
149 selected morphometric parameter through the application of different mathematical procedures
150 (Table 1, serial no.1 to 16). For a consistent comparison, the derived values of the chosen
151 morphometric parameters corresponding to each watershed were subsequently converted to new
152 common evaluation scale of 1-5; on this scale the flood susceptibility increases from 1 to 5.
153 According to the nature of a particular parameter (+ or – relationship with the flood
154 susceptibility), a new value was assigned to each parameter of all the watersheds. Finally, a
155 cumulative value was used to project the flash flood susceptibility of each watershed in the form
156 of a map. The 2nd step was the integration of final flood susceptibility map with two other
157 wetness and surface flow sensitive topographic parameters (Table 1). The two-step approach
158 provided the opportunity to: (i) identify comparative flood hazard of different watersheds and (ii)
159 pinpointing the exact spots within the watersheds displaying higher levels of flash flood
160 susceptibility. The process involved the conversion of all the data layers into raster format, with
161 consistent projection (WGS 1984, UTM Zone 46 N) and cell size (30m x 30m). The use of
162 SRTM digital elevation model (30m) and GIS has been fundamental aspect of this analysis.

163 **4. Results and discussion**

164 *4.1 Morphometric parameters*

165 The basic morphometric characteristics including area (A), perimeter (P) length (Lb), and
166 elevation (m) of the delineated watersheds are presented in the Table 2; and the quantitative
167 analysis of the other parameters and their flash flood connotations are discussed under the
168 respective headings.

169 *4.1.1 Stream order (Su)*

170 The classification of the streams according to number of stream segments (1st, 2nd, 3rd ...) and
171 type of confluence (1st with 1st, 2nd with 2nd, 3rd with 3rd...) is a measure of stream ordering
172 (Strahler, 1957). Su is a fundamental indicator of the size of a drainage basin and discharge
173 capacity. In this analysis watershed B4 and B6 have the highest order of streams (VI), whereas
174 the watersheds including B1, B3, B11, B12, and B13 are with III as the highest order stream
175 (Table 3 and 4). High stream order of B4 and B6 represents presence of larger streams in the
176 catchments fed by multiple small streams, thus having the potential of high water discharge and
177 depending on the relief conditions high flow velocities as well.

178 *4.1.2 Stream number (Nu)*

179 Stream number is the count of streams of different orders in a given drainage basin or a
180 watershed (Strahler, 1957). The watersheds having high stream numbers usually cause high
181 runoff and rapid peak flow during rain storm events than the basins with low Nu (Bhat et al.,
182 2019). The stream number was found to be highest (1934) in watershed B4 (Table 5, Fig 4)
183 followed by B6, B5, and B8 with 950, 260 and 215 respectively. All the remaining watersheds
184 show Nu of less than 200 with lowest being that of the B11 watershed (25), suggesting least
185 runoff capacity.

186 *4.1.3 Stream length (Lu)*

187 Lu refers to the length of streams of different orders in a basin. Stream length is one of the
188 important characteristics of surface runoff; larger Lu is an insinuation of less infiltration and high
189 runoff producing ability of a drainage basin (Strahler, 1952). Lu and Nu are positively related
190 i.e., watersheds with high Lu have high Nu value as well and are thus proxy representatives of
191 each other. As expected from the size of the watershed, B4 revealed highest (1943.93) Lu,

192 followed by B6 (954.64), B8 (302.73), and B5 with 280.03. Similar to the pattern of the Nu, rest
193 of the watersheds have Lu lower than 200 (Table 5 and Fig 4).

194 *4.1.4 Stream Frequency (Fs)*

195 The count of stream segments of all orders per unit area is referred to as stream frequency. High
196 Fs implies high runoff delivery, which is generally a function of impermeable surface material,
197 sparse vegetation cover, and high relief (Patton and Baker, 1976; Reddy et al., 2004). The Fs of
198 the watersheds ranges from 0.80 as lowest for the watershed B9 to 2.33 as highest for the
199 watershed B5 (Table 5, Fig 4); remaining watersheds reveal the intermediate values of the stream
200 frequency.

201 *4.1.5 Drainage Density (Dd)*

202 The spacing between the channels is called as drainage density (Horton, 1932). Dd is calculated
203 as the total length of channels of all orders per unit area divided by the area of a drainage basin.
204 High drainage density is an important indicator of high runoff volumes and rapid flood peaks
205 (Horton, 1932; Patton, 1988; Pallard et al.2009). High Dd is often associated with impermeable
206 soils, sparse vegetation, and mountainous terrain. In this analysis drainage density was found to
207 be highest in watershed B5 with a value of 2.51 (Table 5, Fig 4), thus is likely to produce high
208 runoff; whereas, the Dd values for other watersheds ranges from 1.07 (B3) to 1.37 (B7).

209 *4.1.6 Texture ratio (Rt)*

210 Representing the ratio between total number of streams and perimeter of a basin, the texture
211 ratio (Rt) is a function of lithology, slope, climate, vegetation, and soil type and is classified into
212 four types i.e., coarse (< 4 per km), intermediate (4–10 per km), fine (10–15 per km), and very
213 fine (> 15 per km) (Smith, 1950). The Rt for the watershed B4 and B6 reveal intermediate values

214 of 7.48 and 5.62 respectively, thus suggesting higher quick peak discharge generation potential
215 (Table 5, Fig 4). The remaining watersheds express coarser texture with lowest being that of
216 watershed 12 with 1.02.

217 218 *4.1.7 Bifurcation ratio (Rb)*

219 Rb is a dimensionless measure representing the ratio between the number of stream segments of
220 any order (Nu) and the next higher order (Nu+1). This is a very important parameter that
221 expresses the degree of ramification of the drainage network (Mesa, 2006). Bifurcation ratio is
222 usually minimum in flat or rolling drainage basins and higher in mountainous or dissected
223 drainage basins (Horton, 1945). Here, the mean bifurcation ratio of the watershed B4 has been
224 observed to be highest (6.09), followed by the B13, and B6 with 4.9 and 4.39 correspondingly.
225 The watershed B1 exhibited a minimum Rb value of 0.67 (Table 5, Fig 4). The high Rb suggests
226 a basin having high runoff generation potential with relatively minimum lag for triggering the
227 flash flooding during torrential rains (Chorley 1969; Howard, 1990).

228 229 *4.1.8 Basin relief (Hr)*

230 Basin relief is the difference in elevation between the lowest and highest points in a basin
231 (Schumm 1956). Basin relief is an important indicator of denudation, landform evolution, and
232 runoff of a watershed (Patton, 1988). Hr also explains the gradient of the streams, slope
233 steepness and precipitous discharge delivery (Hadley and Schumm 1961). The watershed B4
234 (889), B6 (629), B8 (384) and B13 (244) have the high basin relief value connoting higher
235 probability of the flash floods than other watersheds with Hr of less than 100 (Table 5 and Fig 4).

236 237 *4.1.9 Relief Ratio (Rr)*

238 Rr is a ratio of basin relief or total relief to horizontal distance along the longest dimension of the
239 basin parallel to the principal drainage line (Schumm, 1956). Relief ratio allows comparisons of
240 relative relief in basins regardless of differences in scale of topography (Costa, 1987). Rr
241 provides an idea about the flow velocity, slope steepness, and erosion status of a drainage basin.
242 The Rr of the watersheds varies from 21.98 (highest) for B13 to 3.34 (lowest) for B7 (Table 5
243 and Fig 4). The high Rr indicates reduced lag time, sudden peak discharge, and high probability
244 of flash flooding (Patton, 1988).

245 *4.1. 10 Ruggedness number (Rn)*

246 Ruggedness number is the dimensionless product of drainage density and relief (Costa, 1987).
247 Rn is high in the basins with steep long slopes, favoring erosion, quick peak flows and flash
248 floods (Patton and Baker, 1976). A ruggedness < 1 means flat topography; a value of 1–2
249 indicates undulating topography, and extreme values (> 2) indicate ‘badland’ topography (Adnan
250 et al., 2019). Watershed B4 has a highest ruggedness number of 1.125 and the number is less
251 than one in all other watersheds (see Table 5 and Fig 4).

252

253 *4.1. 11 Time of concentration (Tc)*

254 Time parameters such as time of concentration, the time to peak, and the lag time are important
255 considerations in flood hydrology (McCuen et al., 1984). The time of concentration is the
256 maximum time required for water to travel from the most distant point of the watershed to outlet.
257 Tc is a fundamental parameter to calculate the peak discharge potential of a watershed. With

258 inverse relationship, the larger values of the T_c imply lower probability of sudden peak flows.
259 The T_c of the watershed B4 and B6 has been calculated as 57 and 31 respectively (Table 5 and
260 Fig 5). For all other watersheds T_c is less than 30 (calculated after Kirpich, 1940).

261 *4.1.12 Infiltration number (I_f)*

262 The infiltration number is a function of the D_d and F_s . It is an important parameter to understand
263 infiltration potential of a watershed. Higher the I_f , lower will be the infiltration and the higher
264 runoff (Bhatt and Ahmed, 2014). The I_f is lowest in watershed B9 with a value of 0.96,
265 suggesting relatively minimum infiltration, whereas the value is highest (5.84) for the watershed
266 B5 (see Table 5 and Fig 5).

267 *4.1.13 Form factor (F_f)*

268 Form factors is expressed as a ratio between the area of the basin and the square of the basin
269 length (Horton, 1932). Form factor is a parameter to predict the flow intensity of a watershed; the
270 high F_f values indicate high discharge of short duration and vice versa (Gregory and Walling,
271 1973). The watershed B11 is having the highest form factor value of 0.645, followed by the B8
272 an B3 with 0.500 and 0.426 respectively (Table 5 and Fig 5).

273

274 *4.1.14 Topographic Wetness Index (TWI)*

275 TWI is used to calculate topographic control on wetness and runoff (Schmid and Persson, 2003;
276 Sørensen et al., 2006, Wu et al., 2016). Runoff generation can be modelled using the topographic
277 wetness index; the part of a catchment where the wetness index exceeds some threshold is

278 assumed to be saturated (Woods and Sivapalan, 1997). The index allows the delineation of a
279 portion of the watersheds potentially exposed to flood inundation or flash flooding (Risi et al.,
280 2018). In this analysis TWI values range from 1-9, where 1 represents least likelihood of
281 inundation and 9 highest. Although, all the watersheds share a substantial area with high TWI
282 values, the maximum of the area with high TWI values were observed in the watershed B4, B6,
283 B7 and B8.

284 *4.1.15 Topographic Position Index (TPI)*

285 TPI compares the elevation of each cell in a DEM to the mean elevation of a specified
286 neighborhood around that cell (Weiss, 2001). Positive TPI values indicate that the central point
287 is located higher than its average surroundings, while negative values indicate a position lower
288 than the average; TPI is increasingly used to measure topographic slope positions and to
289 automate landform classifications (Reu et al., 2013). Here, we make use of TPI to identify ridges,
290 peaks, flat areas and topographic depressions. Choosing a threshold of -8.10 to 9.59, we identify
291 the areas where probability of waterlogging is relatively high. In general, the steep mountainous
292 parts of the watershed B4, B6 and B8 have least potential to cause topographic inundation than
293 the low relief areas of the other watersheds.

294 *4.2 Flash flood susceptibility mapping*

295 On the basis of cumulative value derived through the adopted methodology, this analysis reveals
296 that B4 and B6 have the high discharge generating potential and are most susceptible to flash
297 floods than the remaining watersheds. The watersheds are spread over 1525.4 km² (B4) and
298 774.9 km² (B6), which collectively constitutes 72.61% of the total area (Fig 6a). The
299 morphometric parameters such as stream number (Nu), stream length (Su), texture ratio (Rt)
300 mean bifurcation ratio (Rb), basin relief (Hr), relief ratio (Rr) and ruggedness number (Rn) with

301 values of 1934, 950 (Nu), 1943.93, 954.64 (Lu), 7.48, 5.62 (Rt), 6.09, 4.39 (Rb), 889, 629 (Hr),
302 9.19, 12.21 (Rr), and 1.125, 0.725 (Rn) for the watershed B4 and B6 respectively have been
303 decisive in determining their 'very high' flash flood susceptibility. The watershed B5 reveals
304 'high' susceptibility (6.95%), followed by B8, and B13 with 'moderate' levels of the
305 susceptibility (8.63%). Watershed B2, B10, B11 exhibit 'low' (4.64%); while as, the remaining
306 watersheds that include B1, B3, B7, B9 and B12 express comparatively least 'very low'
307 susceptible (7.18%) to the flash floods (Fig 6a).

308 Combining the watershed level susceptibility scenario (Fig 6a) with in situ TWI and TPI results
309 (Fig 6b, c) through the procedure of weighted overlay analysis in GIS allowed to precisely depict
310 the flash flood susceptibility of each spot (30x30m pixel) in all the watersheds (Fig 7). The
311 detailed quantification of the area under various flash flood susceptibility classes in each
312 watershed is presented in Fig 8.

313 In general, all the communities in the study area are exposed to the varying degree of flash
314 flood hazard; but those in the high susceptibility zones of different watersheds have higher
315 probability of being effected. Coincidentally, larger part of the high susceptibility areas in these
316 watersheds is uninhabited and pose limited threat, except the western parts of Chakaria and
317 Cox's Bazar-S. However, given the vulnerability factors such as high population density and
318 fragile nature of the makeshift settlement (Fig. 9), the Rohingya refugees even if located in
319 largely low susceptible watersheds (B9, B10, B11, and B13) seem to be at higher risk of the flash
320 floods. Because of the relatively less rugged terrain and low elevation of the hills in these
321 watersheds, the Rohingya refugee settlements may not be impacted by the high velocity flows
322 but the likelihood of getting inundated during the flash floods is relatively high.

323

324 **5 Conclusion**

325 Each year rainfall induced flash floods cause huge loss of life and property across the globe.
326 Recognizing the flash flood potential of the drainage basins is important for reducing the
327 associated damages. In this study, multiple morphometric parameters effecting runoff volume,
328 flow velocity, and water depth were evaluated for understanding the flash flood susceptibility of
329 thirteen watersheds in SE Bangladesh. The morphometric parameters were derived from the
330 digital elevation model using GIS. The results reveal that watershed B4 and B6 would be more
331 responsive to high intensity rainfall events and may generate larger and instant discharge,
332 suggesting that the watersheds are more susceptible to flash floods than the remaining
333 watersheds considered for this analysis. In addition to general watershed scale morphometric
334 characteristics, consideration of the local topographic effects helped to precisely map the flash
335 flood susceptibility in all watersheds, which also describes the uniqueness of this study.
336 However, vertical accuracy of the basic data set used i.e., 30m SRTM DEM (RMSE = 8.28m) is
337 a major concern here that restricts practical application of the produced results at a scale
338 demanding finer details. Moreover, validation of the derived flood hazard scenarios remained
339 unperformed because of the insufficient historical record of the flash floods. It is also pertinent to
340 point out that flash flood hazard is not entirely a function of morphometric conditions; therefore,
341 the scenarios may change owing to the influence of other factors such as land use/cover and
342 flood management practices in each watersheds and hydraulic structures along the channels.
343 Furthermore, the factors like soil saturation and debris load, though not within the scope of the
344 present analysis are important factors that influence discharge, flow velocity and severity of the
345 flash floods. Despite the limitations and uncertainties of the data and adopted methods, the
346 deliverables of this study hold substantial value for understanding flood hydrology and
347 developing the flood mitigation policy for the study area.

348

349 **Acknowledgements**

350 This research is funded by the Royal Society as part of the project, “Resilient Futures for the
351 Rohingya Refugees” (Award Reference: CHL\R1\180288), supported under the UK
352 Government's Global Challenges Research Fund.

353 The authors are indebted to the editors and the reviewers for their valuable time to review the
354 manuscript and for providing constructive comments that improved the quality and structure of
355 this paper. Free access to the huge archives of satellite data by the NASA is commendable.

356

357

358 **References**

359 Abuzied S., Yuan M., Ibrahim S., Kaiser M, Saleem T. (2016). Geospatial risk assessment of
360 flash floods in Nuweiba area, Egypt. *Journal of Arid Environments*. 133, 54-72.

361

362 ACAPS (2014). Briefing Note – 27 August 2014, North Bangladesh: Floods

363 Adnan M. S. G, Dewan A., Khatun E. Zannat K. E. and Abdullah A. Y. M. (2019). The use of
364 watershed geomorphic data in flash flood susceptibility zoning: a case study of the
365 Karnaphuli and Sangu river basins of Bangladesh. *Natural Hazards*,
366 doi.org/10.1007/s11069-019-03749-3.

367

368 Ahmed B., Rahman M. S., Sammonds P., Islam R. and Uddin K. (2020). Application of
369 geospatial technologies in developing a dynamic landslide early warning system in a
370 humanitarian context: the Rohingya refugee crisis in Cox's Bazar, Bangladesh,
371 *Geomatics, Natural Hazards and Risk*, 11:1, 446-468, DOI:
372 10.1080/19475705.2020.1730988.

373

374 Ahmed B., Orcutt M., Sammonds P., Burns R., Issa R., Abubakar I., Devakumar D. (2018).
375 Humanitarian disaster for Rohingya refugees: impending natural hazards and worsening
376 public health crises. *The Lancet*, 6.

377

378 Alam A., Bhat M. S., Ahmad B., Farooq H., Ahmad S., Sheikh A. H. (2018). Flood risk
379 assessment of Srinagar city in Jammu and Kashmir, India. *International Journal of*
380 *Disaster Resilience in the Built Environment*, 9, 2, DOI 10.1108/IJDRBE-02-2017-0012.

381 Alam A., Sammonds P., Ahmed B. (2019). Cyclone Risk Assessment of the Cox's Bazar and
382 Rohingya Refugee Camps in southeast Bangladesh. *Science of the Total Environment*,
383 704, 135360, <https://doi.org/10.1016/j.scitotenv.2019.135360>.

- 384 Alam A., Bhat M.S. and Maheen M (2019b). Using Landsat satellite data for assessing the land
 385 use and land cover change in Kashmir valley. *GeoJournal*,
 386 <https://doi.org/10.1007/s10708-019-10037-x>.
- 387 Altaf F., Meraj G. and Romshoo S. A. (2013). Morphometric Analysis to Infer Hydrological
 388 Behaviour of Lidder Watershed, Western Himalaya, India. *Geography Journal*.
 389 <https://doi.org/10.1155/2013/178021>.
- 390 Angillieri M. Y. E. (2008). Morphometric analysis of Colanguil river basin and flash flood
 391 hazard, San Juan, Argentina. *Environ Geol*, 55, 107–111, DOI 10.1007/s00254-007-
 392 0969-2
- 393
- 394 Beven, K.J. and Kirkby, M. J. (1979). "A physically based, variable contributing area model of
 395 basin hydrology". *Hydrological Science Bulletin*. 24 (1): 43–69.
 396 doi:10.1080/02626667909491834.
- 397 Bhat M. S., Alam A., Ahmad S., Farooq H. Ahmad B. (2019). Flood hazard assessment of upper
 398 Jhelum basin using morphometric parameters. *Environmental Earth Sciences* 78:54,
 399 <https://doi.org/10.1007/s12665-019-8046-1>.
- 400
- 401 Bhatt S. and Ahmed S.A. (2014) Morphometric analysis to determine floods in the Upper
 402 Krishna basin using Cartosat DEM, *Geocarto International*, 29:8, 878-894,
 403 doi:10.1080/10106049.2013.868042.
- 404
- 405 Borga M., Gaume E., Creutin J. D. and Marchi L. (2008). Surveying flash floods: gauging the
 406 ungauged extremes *Hydrological Processes*, 22, 3883–3885.
- 407 Brammer H (1990). Floods in Bangladesh. *Geographic background to the 1987 and 1988 floods*.
 408 *The Geographical Journal*, 156, 1, 12-22.
- 409 BRCS (2019). Bangladesh Red Crescent Society. Bangladesh: Monsoon Flood 2019 Situation
 410 Report 5 (Date: 19 July 2019)
- 411 Chorley R.J. (1969) *Introduction to fluvial processes*. Methuen and Co. Limited, London, p 588
- 412
- 413 Choudhury M. and Haque E. (2016). We are more scared of the power elites than the floods’’:
 414 Adaptive capacity and resilience of wetland community to flash flood disasters in
 415 Bangladesh. *International Journal of Disaster Risk Reduction*, 19, 145-158.
- 416 Costa J. E. (1987). Hydraulics and basin morphometry of the largest flash floods in the
 417 conterminous United States. *Journal of Hydrology*, 93, 313-338.
- 418 Destro E., Amponsah W., Nikolopoulos E. I., Marchi L., Marra F., Zocatelli D., Borga M.
 419 (2018). Coupled prediction of flash flood response and debris flow occurrence:
 420 Application on an alpine extreme flood event. *Journal of Hydrology* 558, 225–237.
 421
- 422 Farhan Y., Anbar A., Enaba O., Al-Shaikh N. (2015). Quantitative analysis of geomorphometric
 423 parameters of Wadi Kerak, Jordan, using Remote Sensing and GIS. *Journal of Water
 424 Resource and Protection*, 7, 456-475, <http://dx.doi.org/10.4236/jwarp.2015.76037>

- 425
426
427 Risi D. R., Jalayer F., De Paola F., Lindley S. (2018). Delineation of flooding risk hotspots based
428 on digital elevation model, calculated and historical flooding extents: the case of
429 Ouagadougou. *Stoch Environ Res Risk Assess*, 32:1545–1559.
430
- 431 Dewan, A. M., Nishigaki, M., and Komatsu, M. (2003). Floods in Bangladesh: A comparative
432 hydrological investigation on two catastrophic events. *Journal of the Faculty of
433 Environmental Science and Technology*, Okayama University press, 8, 1, 53-62.
434
- 435 Faniran A. (1968). The index of drainage intensity – a provisional new drainage factor. *Aust J
436 Sci.* 31:328–330.
437
- 438 Fenta A. A., Yasuda H., Shimizu K., Haregeweyn N., Woldearegay K. (2017). Quantitative
439 analysis and implications of drainage morphometry of the Agula watershed in the semi-
440 arid northern Ethiopia. *Appl Water Sci* (2017) 7:3825–3840, doi 10.1007/s13201-017-
441 0534-4
442
- 443 Gaume et al., (2009). A compilation of data on European flash floods. *Journal of Hydrology*,
444 367, 1–2, 70-78.
- 445 Gregory K.J., Walling DE (1973) *Drainage basin form and process: a geomorphological
446 approach*. Wiley, New York, p 456
447
- 448 GSB (1990). *Geological Map of Bangladesh*, by Md. Khurshid Alam, A.K.M. Shahidul Hasan,
449 and Mujibur Rahman Khan (Geological Survey of Bangladesh), and John W. Whitney
450 (United States Geological Survey), scale 1:1,000,000, published by Geological Survey
451 of Bangladesh in 1990.
452
- 453 Guisan, A., S.B. Weiss, and A.D. Weiss. (1999). GLM versus CCA spatial modeling of plant
454 species distribution. *Plant Ecol.* 143:107–122, doi:10.1023/A:1009841519580.
455
- 456 Hadley R.F., Schumm S.A. (1961). Sediment sources and drainage basin characteristics in upper
457 Cheyenne River Basin. *U.S. Geological Survey Water-Supply Paper 1531-B*, 198 pp
458
- 459 HCTT (2015). *Flash Floods in Cox’s Bazar, Bandarban and Chittagong Districts June-July 2015*.
460 Bangladesh, HCTT Joint Needs Assessment (JNA).
461
- 462 Horton R.E. (1932) Drainage basin characteristics. *Trans Am Geophys Union* 13:350–361.
463
- 464 Horton R.E. (1945) Erosional development of streams and their drainage basins; hydrophysical
465 approach to quantitative morphology. *Bull Geol Soc Am* 56:275–370.
466
- 467 Howard A.D. (1990). Role of hypsometry and planform in basin hydrologic response. *Hydrol
468 Process* 4(4):373–385
469

- 470 Kamal A.S.M. M., Shamsudduha M., Ahmed B., Hassan S.M. K., Islam M. S., Kelman I., F.
471 Maureen (2018). Resilience to flash floods in wetland communities of northeastern
472 Bangladesh. *International Journal of Disaster Risk Reduction* 31, 478–488.
- 473 Khalil G. M. (1990). Floods in Bangladesh: A question of disciplining the rivers. *Natural*
474 *Hazards*, 3, 379-401.
- 475 Kirpich, Z. P. (1940). Time of concentration of small agricultural watersheds. *Journal of Civil*
476 *Engineering*, 10(6), 362.
- 477 Marchi L., Borga M., Preciso E., Gaume E., (2010). Characterisation of selected extreme flash
478 floods in Europe and implications for flood risk management. *Journal of Hydrology*, 394,
479 1–2, 118-133.
- 480 Melton M.A. (1957) An analysis of the relations among elements of climate, surface properties,
481 and geomorphology, Technical Report No. 11, Office of Naval Research Project NR
482 389-042. Department of Geology, Columbia University, New York.
483
- 484 McCuen R. H., Wong S.L. and Rawls W. J. (1984). Estimating urban time of concentration. *J.*
485 *Hydraul. Eng.*, 1984, 110, 7, 887-904.
- 486 Meraj G., Khan T., Romshoo S.A., Farooq M., Rohitashw K., Sheikh B.A. (2019). An
487 Integrated Geoinformatics and Hydrological Modelling-Based Approach for Effective
488 Flood Management in the Jhelum Basin, NW Himalaya. *Proceedings*, 7, 8.
489 <https://doi.org/10.3390/ECWS-3-05804>.
- 490 Mesa L. M. (2006). Morphometric analysis of a subtropical Andean basin (Tucumán, Argentina).
491 *Environmental Geology*, 50, 8 pp 1235–1242.
- 492 Miller VC. 1953. A quantitative geomorphic study of drainage basin characteristics in the Clinch
493 Mountain area. Virginia and Tennessee, Proj. NR 389-402,
494
- 495 Mirza M. M. Q. (2002). Global warming and changes in the probability of occurrence of floods
496 in Bangladesh and implications. *Global Environmental Change* 12, 127–138.
497
- 498 Ozdemir H. and Bird D. (2009). Evaluation of morphometric parameters of drainage networks
499 derived from topographic maps and DEM in point of floods. *Environ Geol* 56, 1405–1415.
500 doi 10.1007/s00254-008-1235-y
501
- 502 Pallard B, Castellarin A, Montanar A (2009) A look at the links between drainage density and
503 flood statistics. *Hydrol Earth Syst Sci* 13:1019–1029.
504
- 505 Patton, P.C. and Baker, V.R., 1976. Morphometry and floods in small drainage basins subject to
506 diverse hydrogeomorphic controls. *Water Resour. Res.*, 12:941 952.
507
- 508 Patton PC. (1988). Drainage basin morphometry and floods. In: Baker VR, Kochel RC, Patton
509 PC, editors. *Flood geomorphology*. New York (NY): Wiley; p. 51–65.
510

- 511 Philip et al., (2019). Attributing the 2017 Bangladesh floods from meteorological and
512 hydrological perspectives. *Hydrol. Earth Syst. Sci.*, 23, 1409–1429.
513
514
- 515 Reddy G.P.O, Maji A.K, Gajbhiye KS (2004). Drainage morphometry and its influence on
516 landform characteristics in a basaltic terrain, Central India—a remote sensing and GIS
517 approach. *Int J Appl Earth Observ Geoinf* 6(1):1–16
518
- 519 Reu De J. and others (2013). Application of the topographic position index to heterogeneous
520 landscapes. *Geomorphology*, 186, 39–49, doi: 10.1016/j.geomorph.2012.12.015
521
- 522 Romshoo S. A., Bhat S. A. and Rashid I. (2012). Geoinformatics for assessing the morphometric
523 control on hydrological response at watershed scale in the Upper Indus Basin. *J. Earth*
524 *Syst. Sci.* 121, 3, 659–686
525
- 526 Schmidt, F. and Persson, A. (2003). Comparison of DEM Data Capture and Topographic
527 Wetness Indices Precision Agriculture. 4: 179.
528 <https://doi.org/10.1023/A:1024509322709>.
529
- 530 Schumm S.A (1956). Evolution of drainage system and slope in badlands of Perth Amboy, vol
531 67. Geological Society of America Bulletin, New Jersey, p 597
532
- 533
- 534 Smith K.G. (1950) Standards for grading texture of erosional topography. *Am J Sci* 248:655–
535 668.
536
- 537 Sørensen, R., Zinko, U., and Seibert, J. (2006) On the calculation of the topographic wetness
538 index: evaluation of different methods based on field observations, *Hydrol. Earth Syst.*
539 *Sci.*, 10, 101-112, <https://doi.org/10.5194/hess-10-101-2006>.
- 540 Strahler A. N. (1952). Hypsometric (area-altitude) analysis of erosional topography. *Bull Geol*
541 *Soc Am* 63:1117–1142. [https://doi.org/10.1130/0016-7606\(1952\)](https://doi.org/10.1130/0016-7606(1952)).
542
- 543 Strahler A.N. (1957) Quantitative analysis of watershed geomorphology *Eos. Trans Am*
544 *Geophys Union* 38:913–920, doi.org/10.1029/TR038 i006p 00913
545
- 546 Tarannum T. (2018). Case Study of Flash Flood in Bangladesh, 2017. In *South Asia Flash Flood*
547 *Guidance System (SAsiaFFGS) Follow-up Operational Workshop (Step 4 training)*, New
548 *Delhi, India, 5-7 June 2018*.
549
- 550 UNHCR (2019). Bangladesh Refugee Emergency. Population Fact Sheet.
- 551 Weiss, A. D. (2001). Topographic position and landform analysis. Poster presentation, ESRI
552 *User Conference, San Diego, California, USA*.
553

- 554 Woods R. A. and Sivapalan M. (1997). A connection between topographically driven runoff
555 generation and channel network structure. *Water Resources Research*, 33, 12, 2939-2950.
- 556
- 557 Wu Y., Giri S., Qiu Z. (2016). Understanding the spatial distribution of hydrologic sensitive
558 areas in the landscape using soil topographic index approach. *International Soil and Water*
559 *Conservation Research*. 4, 278–283
- 560 www.dhakatribune.com, [https://www.dhakatribune.com/bangladesh/2019/07/26/flood-death-toll-](https://www.dhakatribune.com/bangladesh/2019/07/26/flood-death-toll-crosses-100-in-two-weeks)
561 [crosses-100-in-two-weeks](https://www.dhakatribune.com/bangladesh/2019/07/26/flood-death-toll-crosses-100-in-two-weeks) (last accessed on 22 September, 2019)
- 562 www.wmo.int: [https://public.wmo.int/en/projects/flash-flood-guidance-system-global-coverage-](https://public.wmo.int/en/projects/flash-flood-guidance-system-global-coverage-gffg)
563 [gffg](https://public.wmo.int/en/projects/flash-flood-guidance-system-global-coverage-gffg) (last accessed on 27 September, 2019)
- 564 <http://floodlist.com/asia/myanmar-bangladesh-rohingya-monsoon-floods-june-2018> (last
565 accessed on 27 September, 2019)

Table 1 Morphometric parameters selected for the present analysis

<i>S. No.</i>	<i>Parameter</i>	<i>Mathematical expression</i>	<i>Reference</i>
1	Basin area (A) km ²	A = the entire area from drainage divide to outlet point	Schumm, 1956
2	Perimeter (P) km	P = the perimeter is the total length of the drainage basin boundary	Schumm, 1956
3	Basin length (L _b) km	L _b = the basin length corresponds to the maximum length of the basin measured parallel to the main drainage line	Schumm, 1956
4	Stream order (S _u)	Hierarchical = classification of streams based on the number and type of tributary junctions	Strahler, 1952
5	Stream number (N _u)	$N_u = N_1 + N_2 + \dots + N_n$	Strahler, 1952
6	Stream length (L _u)	$L_u = L_1 + L_2 + \dots + L_n$	Strahler, 1952
7	Stream frequency (F _s)	$F_s = Nu/A$ where, Nu = total number of stream segments of all orders, and A = basin area.	Horton, 1945
8	Drainage density (D _d)	$Dd = Lu/A$ where, Lu = total length of all the ordered streams, and A = area of the basin.	Horton, 1945
9	Texture ratio (R _t)	$R_t = Nu/P$ where, Nu = total number of stream in a given basin, and P = perimeter of the basin	Smith, 1950
10	Bifurcation ratio (R _b)	$R_b = Nu/N_{u+1}$ where, Nu number of streams of any given order, Nu+1 the number in the next higher order	Horton, 1945
11	Basin relief (H _r)	$H_r = H_{max} - H_{min}$ (m) where H _{max} is the highest and H _{min} the lowest point of the basin	Schumm, 1956
12	Relief ratio (R _r)	$R_r = H_r/L$ R _r is the dimensionless height-length ratio between the basin relief (R) and the basin length (L)	Schumm, 1956
13	Ruggedness number (R _n)	$R_n = Dd \times (Br/1000)$ where, Br = basin relief Dd = drainage density	Melton, 1957
14	Time of concentration (T _c)	$T_c = G k (L / S^{0.5})^{0.77}$ where, G = Constant (G=0.0078) k = Kirpich adjustment factor L = Longest watercourse length in the watershed S = Average slope of the watercourse	Kirpich, 1940
15	Infiltration number (I _f)	$I_f = F_s \times D_d$ where, F _s is stream frequency the and D _d drainage density	Faniran, 1968

16	Form factor (F)	$F = A/L^2$	Horton, 1932
Basin	Area (km ²) (A)	Perimeter (km) (P)	Length (km) (L _b)
17	Topographic Wetness Index (TWI)	$TWI = \ln(a/\tan\beta)$, Where, a is the specific catchment area (SCA): the local upslope area draining through a certain point per unit contour length, which is equal to a certain grid cell width, and β is the local slope	Elevation (m) Min (h) Max (H) Beven and Kirkby, 1979
18	Topographic Position Index (TPI)	$TPI_i = M_0 - \sum_{n=1}^n \frac{M_n}{n}$ where, M_0 = elevation of the model point under evaluation, M_n = elevation of grid, n = the total number of surrounding points employed in the evaluation.	Guisan et al., 1999; Weiss, 2001

Table 2 Basic morphometric attributes of the selected watersheds

B1	26.6	27.5	12.0	1	98
B2	92.4	48.7	15.5	1	97
B3	28.0	32.8	8.1	1	47
B4	1525.4	258.3	96.7	0	889
B5	220.4	85.2	25.8	0	108
B6	774.9	169.0	51.5	0	629
B7	93.0	71.5	22.4	0	75
B8	233.4	93.5	21.6	0	384
B9	61.9	48.5	17.3	0	75
B10	38	33.9	11.2	0	73
B11	16.8	20.4	5.1	1	70
B12	18.1	25.4	8.0	0	57
B13	40	35.5	11.1	0	244

Table 3 Stream order (Su) and Stream number (Nu) of the watersheds

Basin	I	II	III	IV	V	VI	Total
B1	20	11	7	0	0	0	38
B2	73	37	26	6	0	0	142
B3	24	11	5	0	0	0	40
B4	1113	537	265	14	4	1	1934
B5	173	73	10	3	1	0	260
B6	612	299	29	7	2	1	950
B7	78	36	7	1	0	0	122
B8	173	29	10	2	1	0	215
B9	39	8	2	1	0	0	50
B10	35	17	1	0	0	0	53
B11	15	9	1	0	0	0	25
B12	17	8	1	0	0	0	26
B13	35	23	1	0	0	0	59

Basin	I	II	III	IV	V	VI	Total
B1	13.78	7.1	9	0	0	0	29.88

B2	58.93	32.98	21.33	4.38	0	0	117.62
B3	14.92	11.2	3.97	0	0	0	30.09
B4	980.77	495.44	230.17	118.77	62.43	56.35	1943.93
B5	138.74	63.77	59.9	13	4.62	0	280.03
B6	467.23	256.33	115.66	85.57	29	26.95	954.64
B7	644.79	333.58	141.90	14.67	10	0	1274.3
B8	1744.89	905	491.05	11.06	38	0	3012.33
B9	3096	1548	191.05	211	0	0	7543.3
B10	24.41	15.23	9.07	0	0	0	48.71
B11	11.9	6.57	2.38	0	0	0	20.85
B12	15.58	4.99	3.43	0	0	0	24
B13	23.94	17.23	3.7	0	0	0	44.87

Table 4 Stream length of all the orders (Su) in each watershed

B1	38	29.88	1.42	1.12	1.38	0.67	97	8.083	0.097	12	1.59	0.184
B2	142	117.62	1.53	1.27	2.91	1.54	96	6.19	0.104	16	1.94	0.384
B3	40	30.09	1.42	1.07	1.21	0.87	46	5.67	0.033	10	1.51	0.426
B4	1934	1943.93	1.26	1.27	7.48	6.09	889	9.19	1.125	57	1.60	0.163
B5	260	280.03	2.33	2.51	3.05	3.19	108	4.18	0.381	27	5.84	0.167
B6	950	954.64	1.22	1.23	5.62	4.39	629	12.21	0.725	31	1.50	0.292
B7	122	127.43	1.31	1.37	1.70	2.86	75	3.34	0.086	28	1.79	0.185
B8	215	302.73	0.92	1.29	2.29	3.17	384	17.77	0.443	13	1.18	0.500
B9	50	75.33	0.80	1.21	1.03	2.17	75	4.33	0.082	20	0.96	0.206
B10	53	48.71	1.36	1.25	1.56	3.81	73	6.51	0.082	12	1.7	0.310
B11	25	20.85	1.48	1.24	1.22	2.13	69	13.5	0.080	5	1.83	0.645
B12	26	24	1.43	1.32	1.02	2.02	57	7.12	0.027	9	1.88	0.282
B13	59	44.87	1.47	1.12	1.66	4.9	244	21.98	0.256	7	1.64	0.323

Table 5 Derived values of all the morphometric parameters for each watershed

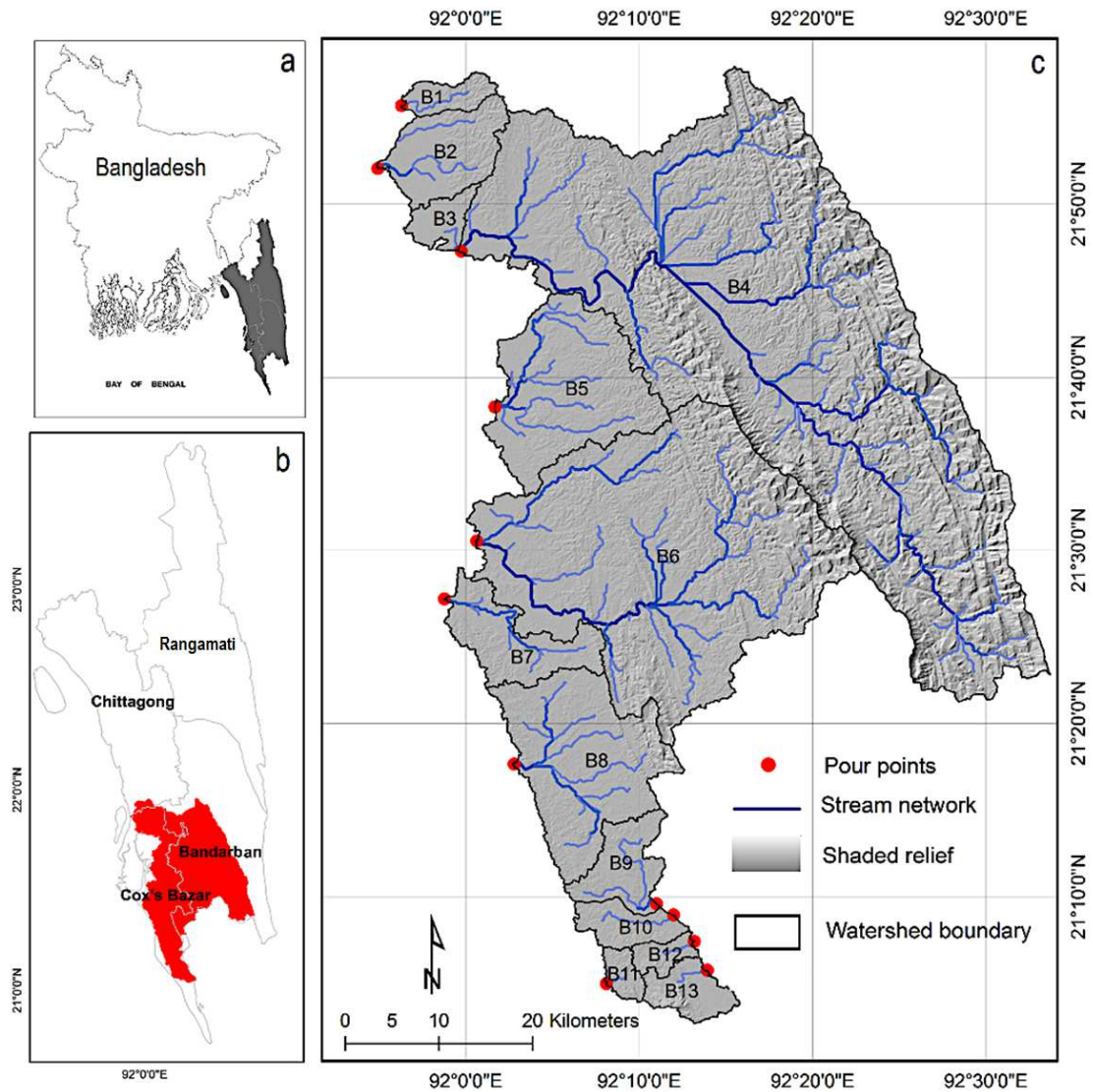


Fig 1 a. Location of the study area in Bangladesh, b. spatial extent of the site in relation to neighbouring sub-districts, and c. shaded relief showing the selected watersheds, drainage divide, major streams and pour point of each watersheds.

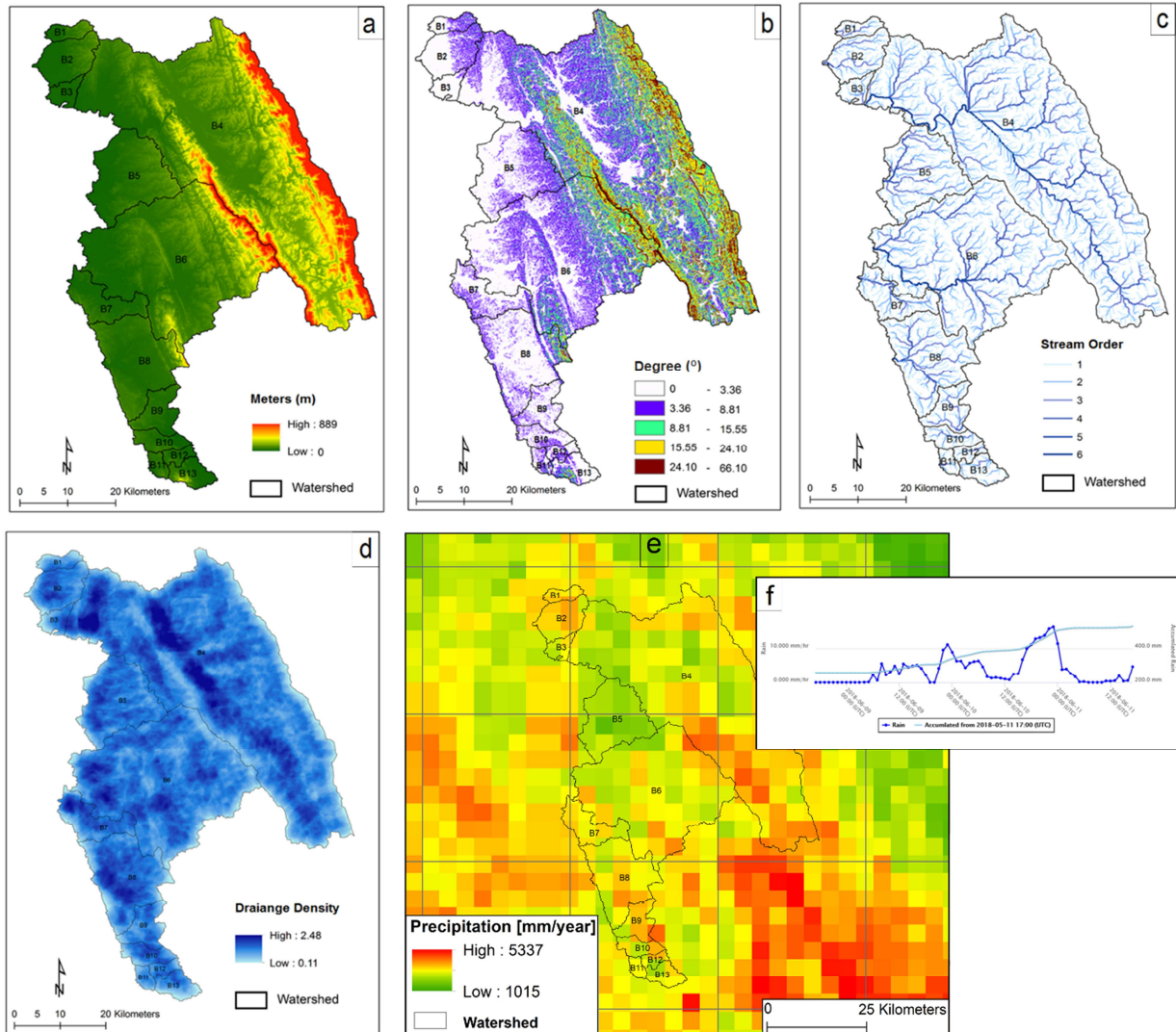


Fig 2 General physical characteristics of the selected watersheds; a. digital elevation model (SRTM 30m), b. slope ($^{\circ}$), c. stream order, d. drainage density, e. precipitation pattern [Tropical Rainfall Measuring Mission (TRMM)] and f. rainfall [Global Rainfall Map (GSMaP)] of June 2018 flash flood.

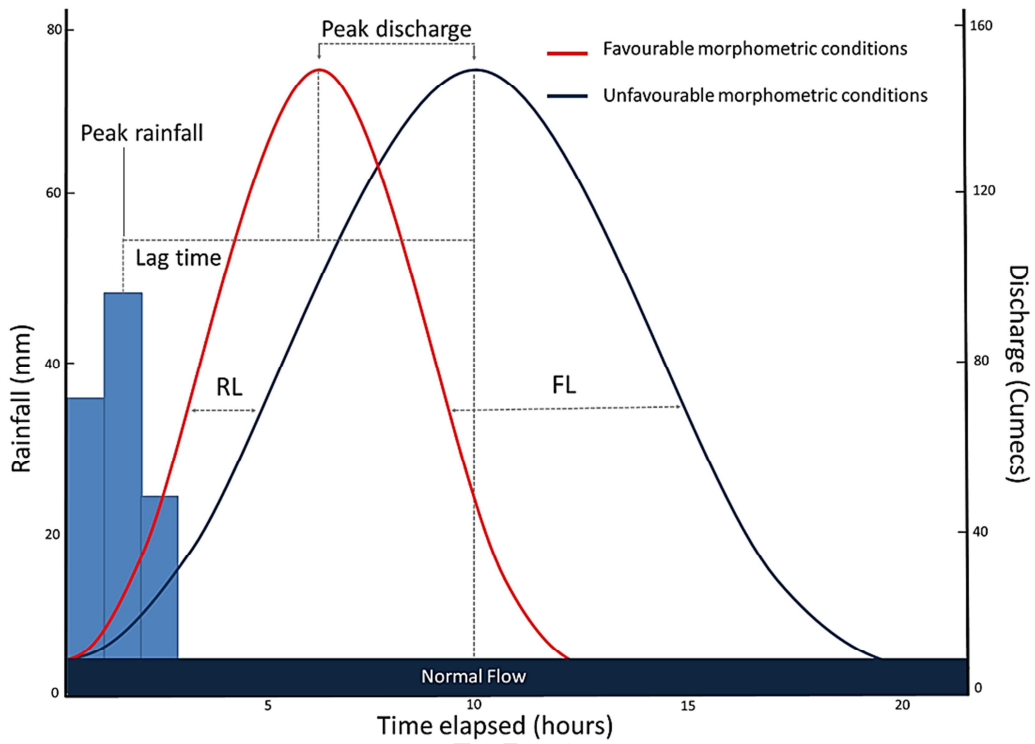


Fig 3 Hydrograph illustrating the general effect of drainage basin morphometry on peak discharge; RL: rising limb, FL: falling limb.

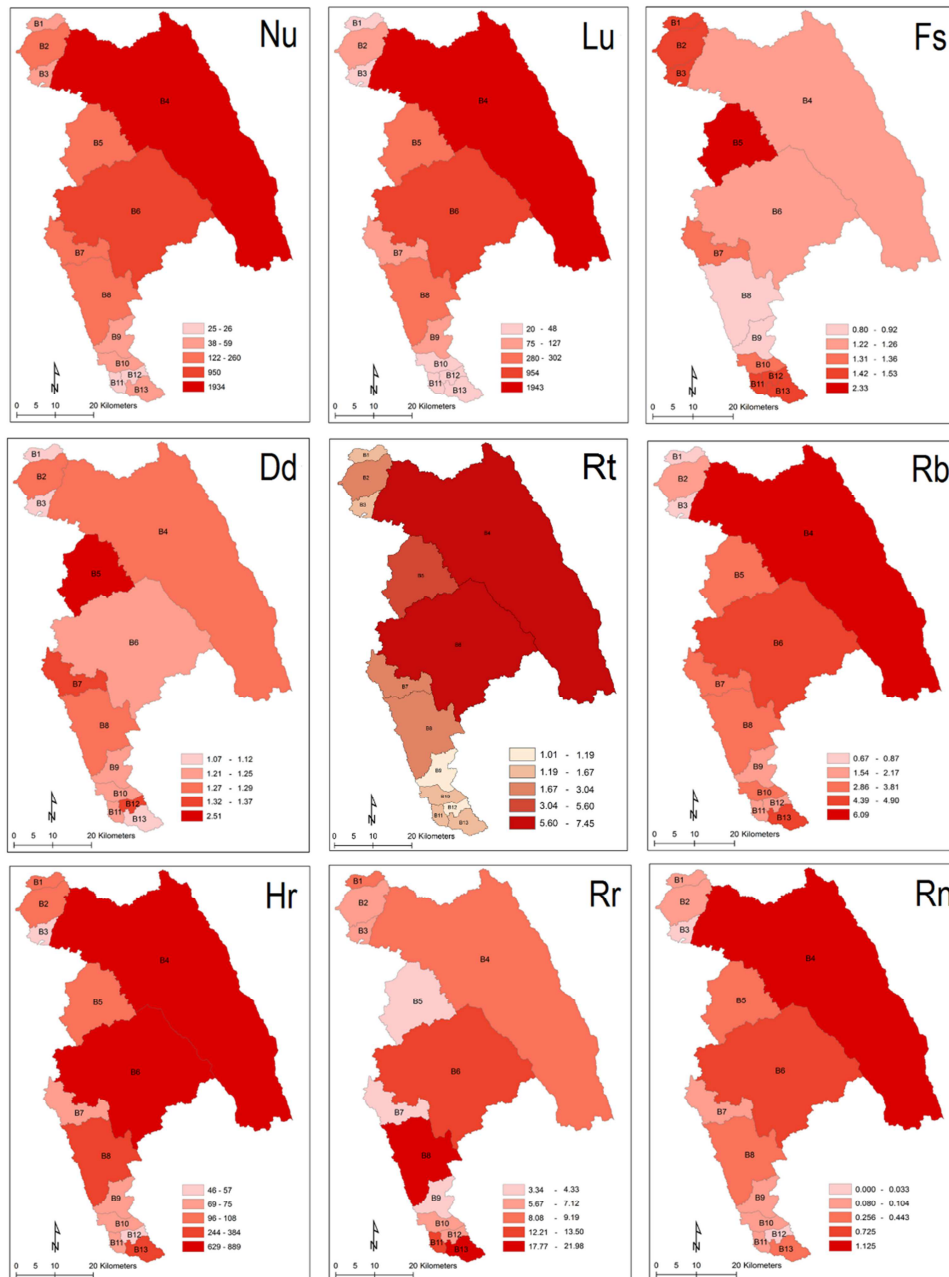


Fig 4 Morphometric parameters; stream number (Nu), stream length (Lu), Stream frequency (Fs), drainage density (Dd), texture ratio (Rt), bifurcation ratio (Rb), basin relief (Hr), relief ratio (Rr), and Ruggedness number (Rn).

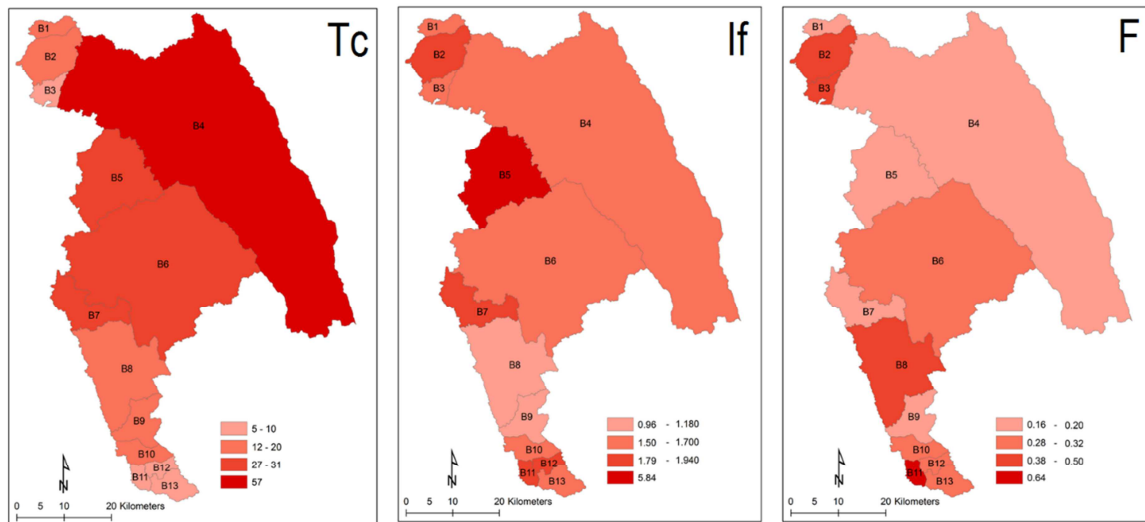


Fig 5 Morphometric parameters; time of concentration (Tc), infiltration number (If), and form factor (F).

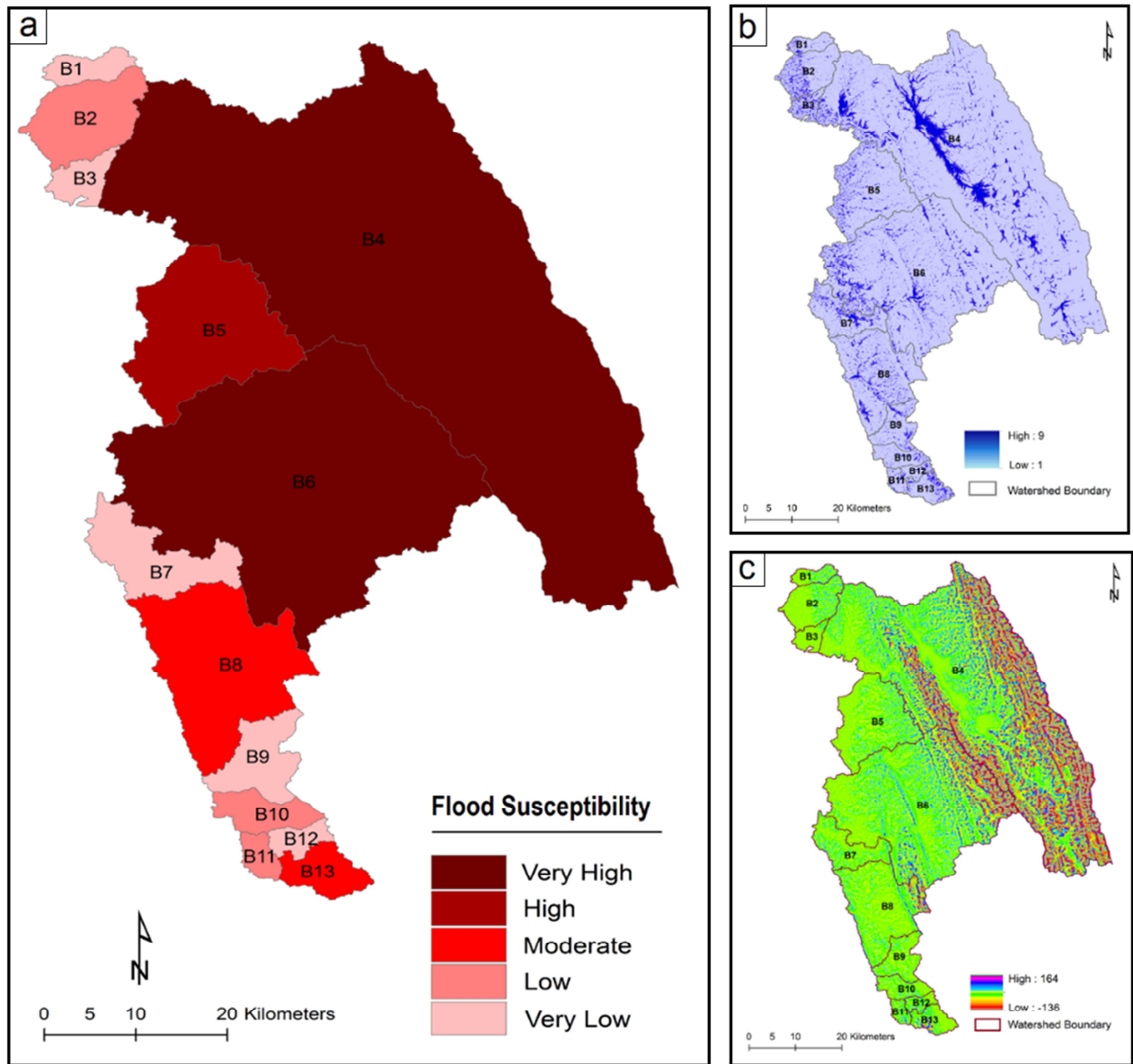


Fig 6 a. Relative flash flood susceptibility of the watersheds, b. topographic wetness index (TWI), c topographic position index (TPI).

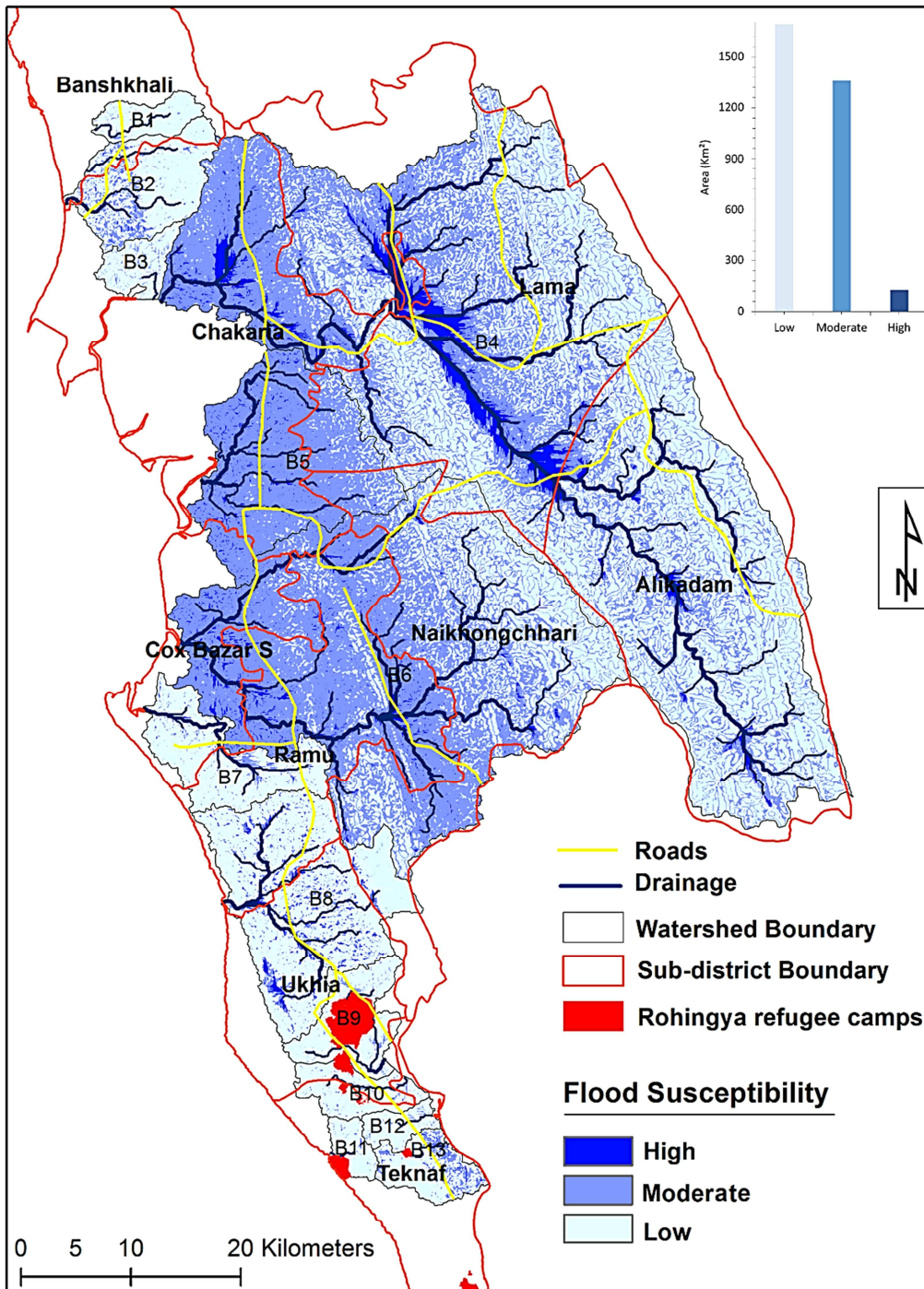


Fig. 7 Precise flash flood susceptibility scenario of all the locations in each watershed.

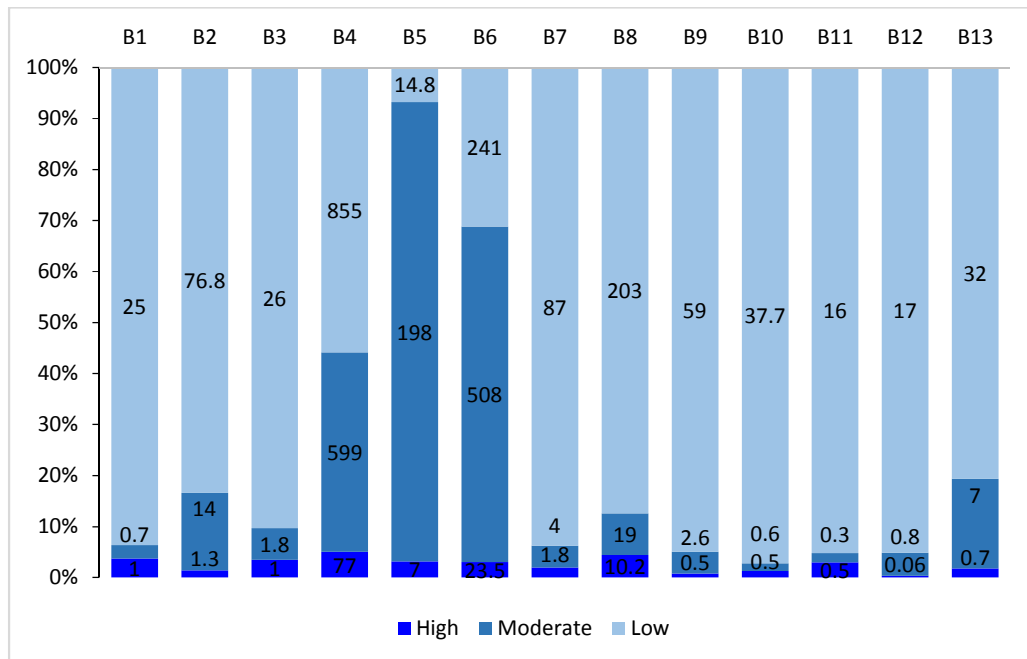


Fig 8 Area under various flash flood susceptibility classes in each watershed (B1-B13); figures are in square kilometers.



Fig. 9 Google Earth images showing the enormous land transformation in the B9 watershed of the study area as result of Rohingya refugee influx from Myanmar; the inset on the 2017 image shows the zoomed view of a part of the Kutupalong refugee camp.

Conflict of Interest

The authors declare no conflict of interest.

Akhtar Alam
On behalf of all authors

Journal Pre-proof